PIC TESTING ON WAFER LEVEL

Automated testing of photonic integrated circuits (PICs) before packaging is crucial to achieve higher throughput. The photonic test prober SIRIUS, developed within a MEKOPP consortium project, offers an automated solution for optical and electrical testing at wafer level. A demonstrator was set up to validate its functionality for wafer testing, while parallel research focused on simplifying the manipulators for the optical probes and collision avoidance for trench coupling.

ROY KELDER

Introduction

The ability to find critical defects at the wafer level avoids expensive packaging processes for photonic integrated circuits (PICs). At the moment, Ph.D. candidates and R&D engineers perform the tests concerned in a lab environment, often relying on time-intensive, manual electrical and optical probing. This approach creates a bottleneck in terms of cost and throughput. To counter these challenges, the MEKOPP consortium, led by IMS, introduces SIRIUS, a photonic test prober that provides the user with an automatic way for optical and electrical testing of PICs on a wafer. The probing solution with SIRIUS has been developed on the same platform as the photonic visual inspection tool HELIOS (see a forthcoming issue of *Mikroniek*).

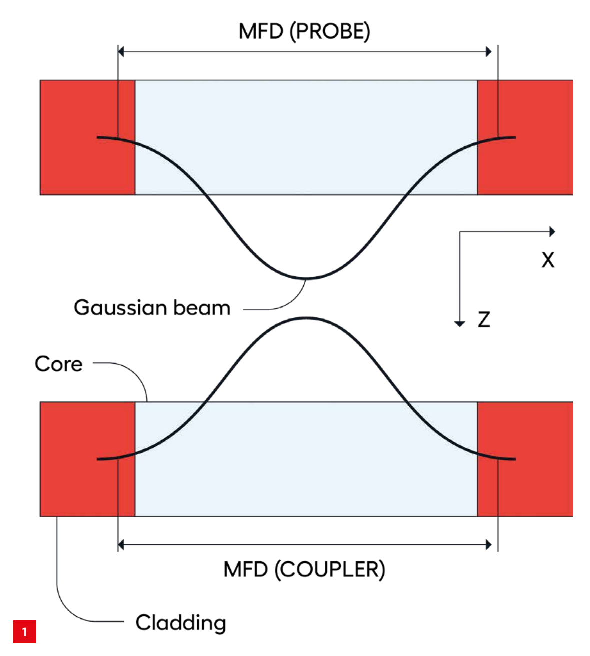

1

Optical probe and coupler modelled as single-mode step-index fibers with symmetrical gaussian beams.

Optical probing of PICs

Functional tests of a PIC require both an electrical and an optical coupling with minimal losses. Alignment techniques that minimise the effect of electrical coupling losses are well-known. Where electrical coupling is achieved by pressing electrical pins to the conducting pads of the PIC, optical coupling for tests is done by positioning optical probes close to couplers. Unlike electrical probing, optical probing is typically done contactless.

The coupler is the interference structure where light is guided into and out of the PIC. A common method to calculate the coupling loss between an optical probe and the coupler is to approximate the emitted light as a Gaussian beam, and calculate the modal overlap between the Gaussian beams. Here, the probe and coupler are both represented as single-mode step-index fibers (as shown in Figure 1).
With this Gaussian approximation, rather concise analytical equations can be derived that describe the relation between optical coupling loss (η) and the various misalignment errors between the probe and coupler [1]:

- varying axial gap (z), with Rayleigh length $z_0 = \pi n \omega^2/\lambda$:

$$\eta_z = \frac{1}{1+\left(\frac{z}{2z_0}\right)^2} \tag{1}$$

- radial misalignment (x):

$$\eta_x = e^{-\frac{x^2}{\omega^2}} \tag{2}$$

- angular misalignment (θ):

$$\eta_\theta = e^{-\frac{(\pi n \omega \theta)^2}{\lambda^2}} \tag{3}$$

Important parameters are the wavelength of the propagating light (λ), the refractive index (n) and the Mode Field Diameter (MFD). The latter can be expressed in the mode radius (ω) as $MFD = 2\omega$.

AUTHOR'S NOTE

Roy Kelder is an R&D engineer at IMS (Integrated Mechanization Solutions), located in Almelo (NL).
IMS develops and builds production automation solutions for small and innovative products, providing solutions that enable world-leading organisations to scale up production by offering robust, modular production equipment and advice.
The author wrote this article with the help of Gerwin Osnabrugge, an optical engineer at PHIX, located in Enschede (NL). The article is partially based on research by graduate interns Anne Heijink and Lex Mulder from the University of Twente, who were supervised by Kelder and Osnabrugge.
The photonic metrology machine development described in this article was led by IMS in the MEKOPP consortium (Metrology Equipment for critical scale up of PIC Production).

jasper.minten@ims-nl.com
www.ims-nl.com/sirius
www.hightechnl.nl/mekopp/projecten/mekopp

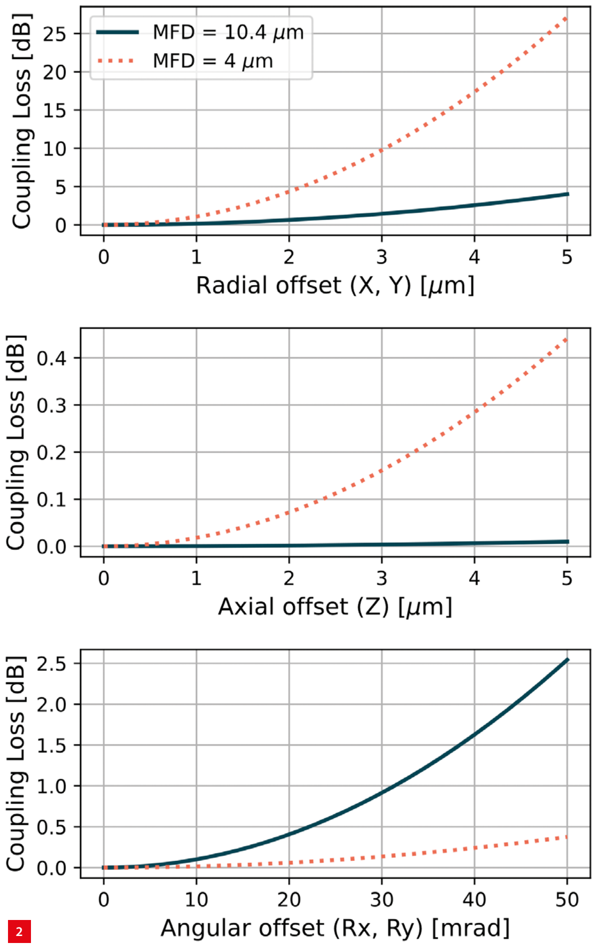

2

Optical coupling losses, in dB using $-10 \cdot \log_{10}(\eta)$*, for different alignment errors. A wavelength of 1,550 nm and refractive index of 1.46 are used.*

From Equations 1 to 3 and Figure 2, it can be observed that a variation in *MFD* has a significant impact on sensitivity. The radial accuracy needs to be higher than the axial accuracy, while angular offset is not critical. Please note, this is valid for a single-I/O optical port with symmetrical Gaussian beams in near-field with matching *MFD* between probe and coupler.

Grating and edge couplers

How to test a PIC at wafer level depends largely on the type of coupler. Currently, the simplest method for wafer level testing is via a grating coupler. Figure 3 illustrates such a coupler that diffracts light into and out of the PIC using a diffraction grating that has been apodised (modified for an optimal signal profile). It exploits periodic variations in the refractive index of the material. If the grating period is in the order of the wavelength of the light, diffraction occurs, causing the light to scatter in different directions. In this way, grating couplers are used to direct the light out of the plane of the wafer towards the optical probe.

Tuning grating couplers (and optical probes) for optimal coupling is a research area in its own right and is not yet standardised. Probing on the SIRIUS is mainly done on an apodised grating with a focusing structure (shown in Figure 4).

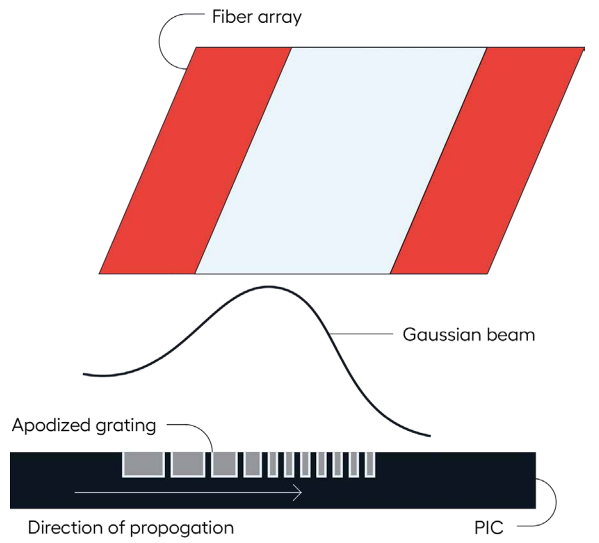

3

Optical probe (as a fiber array) and an apodised grating with approximated Gaussian beam.

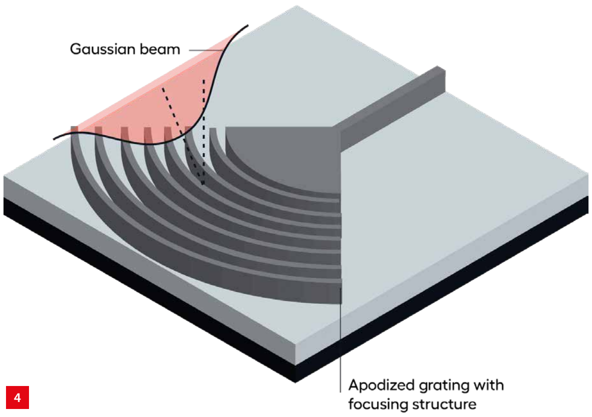

4

Apodised grating coupler with focusing structure and Gaussian beam from an optical probe.

Such structures are optimised for a probe with a Gaussian distribution and a specific angle of incidence of the probe.

An edge coupler is a waveguide designed with a facet at the edge of a PIC, which allows a probe to couple light into it. It functions similarly to how two fibers are aligned and probe against each other for coupling, as shown in Figure 1. Unlike a grating coupler, which couples light out-of-plane, an edge coupler is in-plane. By avoiding the use of the diffraction technique, a broader transmission bandwidth can be achieved, along with a lower coupling loss.

The trench coupling is a special configuration of an edge coupling. On wafer level, deep-etched dicing trenches expose the edges of the PICs. The narrowness of these trenches imposes strict design constraints on the probe type and requires, for some cases, sensing for collision avoidance.

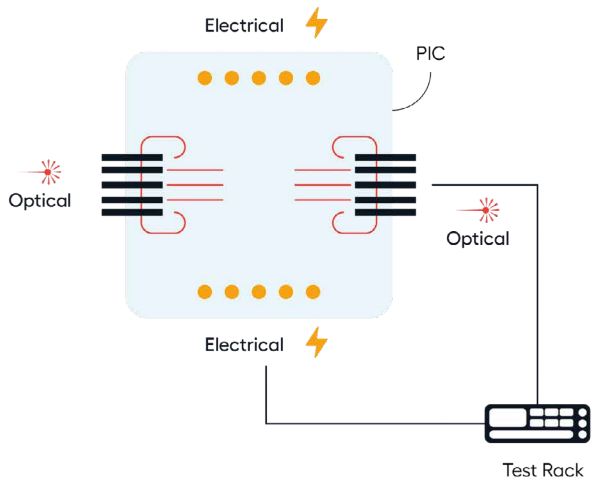

5

Illustration of a probing configuration on the photonic test prober. The top and left side of the PIC are used as input, whereas the bottom and right side are used as output. The test rack is modular and can be equipped with customer-specific hardware for tests.

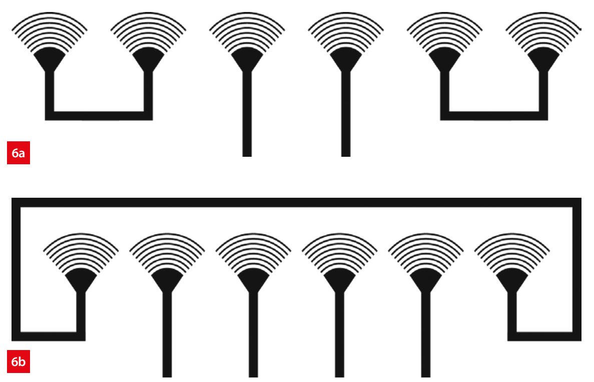

Grating coupler layouts for alignment.
(a) Two pairs of grating couplers.
(b) Outer grating couplers.

Probing configurations

The optical couplers on a PIC, for SIRIUS, are typically positioned on the right and left side, whereas the electrical couplers are on the top and bottom side [2]. A schematic of such a PIC is shown in Figure 5. All sides can be probed simultaneously. SIRIUS supports PICs with up to 2x32 optical couplers of pitch 127 or 250 µm, and up to 3,000 electrical couplers.

The optical probes are actively aligned using gradient-based search algorithms to achieve minimal coupling losses [3]. This requires that the probes are positioned accurately enough to establish optical feedback. The outer couplers are used for optical feedback, while the inner couplers are the functional channels. Typical layouts of grating couplers are shown in Figure 6, with Figure 6a where first light is more easily detected because the probe can have a larger initial tilt-alignment error relative to the couplers. This is due to the use of two pairs of couplers for optical feedback that are close to each other. When first light is more easily established, only one pair of couplers that are far apart needs to be used, as shown in Figure 6b.

When probing into edge couplers, the layout of Figure 6a is most commonly used to circumvent waveguide crossing. Another layout exists where couplers and waveguides are used for both optical feedback and signal transmission. However, the complexity increases due to the multiple degrees of freedom (DoFs) for active alignment and the effect of the feedback passing through the photonic components.

Optical probe types

An optical probe for a PIC with grating couplers consists of multiple fibers arranged in parallel and encapsulated between a substrate and a lid; this is also called a fiber array. The front facet is polished at an angle to match the incident angle of the grating coupler. For edge couplers, the fiber array can be cleaved and polished at an angle of 45° [4]. However, this configuration often results in higher coupling losses due to the additional travel distance of light after reflection on the internal surface. To counter the *MFD* mismatch, 3D-printed periscopes on the fiber array can be used [5] (Figure 7). Another option is using tapered fiber to establish a so-called adiabatic coupling [6].

A promising configuration is to use a probe with alignment fingers, where each finger is passively aligned in etched spaces on the PIC [7]. In this configuration, the probe and the PIC are in physical contact, but the end facets do not touch. To avoid the need for specialised probes for edge coupling, a spot-size convertor can also be integrated directly onto the PIC. This approach reduces the required alignment accuracy, simplifying the probing process.

Photonic test prober SIRIUS

The electrical probe card and optical probes on SIRIUS can be easily swapped within 30 minutes. After the swap, a custom

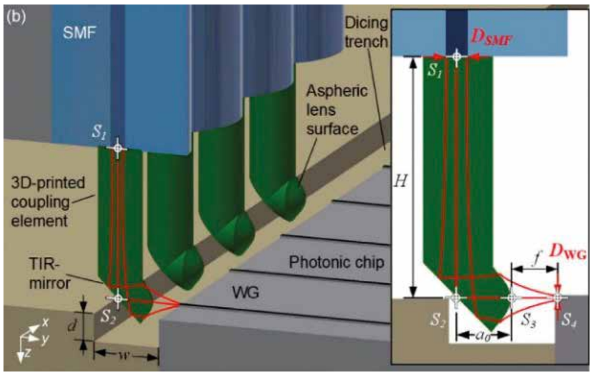

7

Close-up view of a 3D-printed coupling probe, with a deep-etched trench of w ≥ 50 µm and d ≥ 20 µm; WG = Wave Guide. (Image courtesy of [5])

8 The photonic test prober demonstrator with control cabinets in the background.

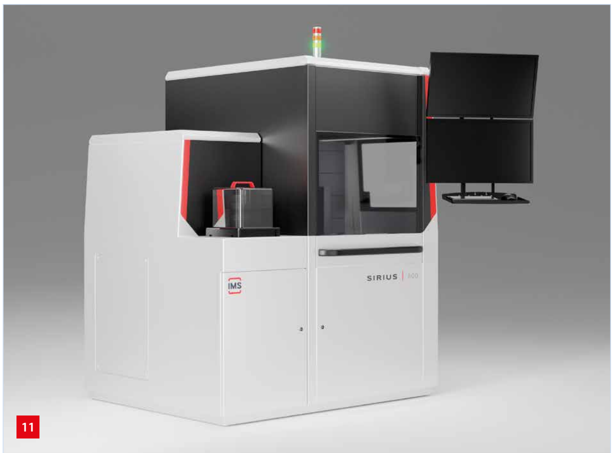

11 Photonic test prober SIRIUS.

9 Close-up of wafer stage, chuck, wafer (blurred), probe card and manipulators with optical probes.

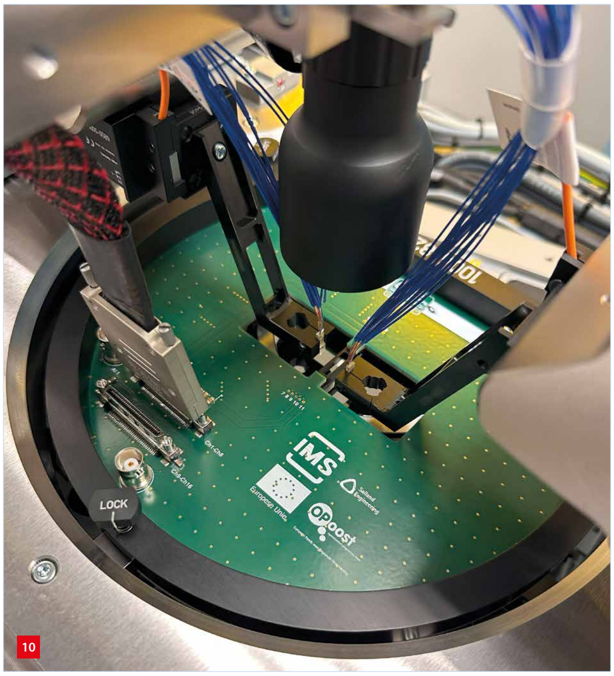

10 Close-up of probe card for electrical I/O and fiber arrays for optical I/O.

recipe can be activated. The system's SECS/GEM (SEMI Equipment Communications Standard/Generic Equipment Model) works with the MES (Manufacturing Execution System) according to the SEMI E30 standard and with specific additions for the test equipment described in SEMI E122. Test protocols, wafer maps, recipes, and test reports can be managed through EZ-MES [8]. A new wafer can be loaded automatically using cassettes or SMIF (Standard Mechanical Interface) pods. A wafer handler transports the wafer to both an ID-recognition scanner and a pre-aligner, which orients the notch correctly. The wafer is transported with the wafer handler to the thermally conditioned chuck of the wafer stage. The chuck is just above ambient temperature to ensure repeatable test conditions between wafers.

An automatic calibration procedure maps the wafer fiducials to the electrical probe card pins and optical probes. After calibration, the wafer is pressed against the electrical tips of the probe card. The two optical probes are both moved with a coarse manipulator to establish first light. To optimise the coupling, a fine-stroke manipulator actively aligns with optical feedback. Then a PIC test can start. Hardware that comes with these tests can be easily integrated in the test rack. Typical instruments are an optical spectrum analyser, a laser source, a broadband source for alignment and optical switches. Photos of the photonic test prober demonstrator can be seen in Figures 8-10. This demonstrator was tested to validate its functionality for wafer probing.
The photonic test prober SIRIUS is shown in Figure 11, while a 360° view was created to offer a better visual representation (see the video, [V1]).

Research

In parallel with the development of the photonic test prober SIRIUS, research has been done at IMS on simplifying the manipulators [9] for grating coupling. Also, research has been performed on collision avoidance [10] for trench coupling when using a periscope probe.

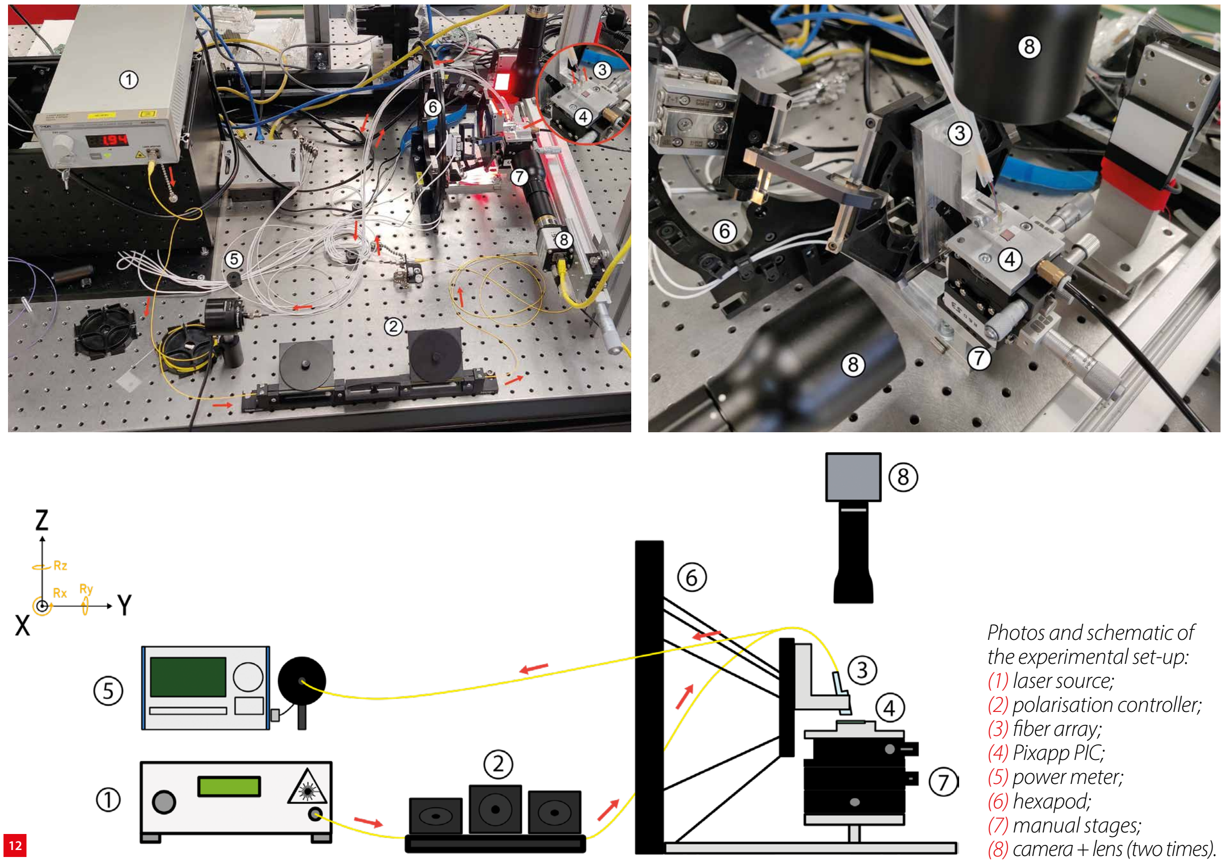

12

Photos and schematic of the experimental set-up:
(1) laser source;
(2) polarisation controller;
(3) fiber array;
(4) Pixapp PIC;
(5) power meter;
(6) hexapod;
(7) manual stages;
(8) camera + lens (two times).

Simplifying the manipulators

The manipulators on the photonic test prober consist of a 6-DoF coarse-alignment hexapod and a 3-DoF fine-alignment piezo in series. For scenarios with minimal PIC-size variation, probing only grating couplers, and a less strict requirement on the coupling loss of 9 dB, a simpler concept is proposed. In this concept, some of the rotational axes are made passive, meaning they are mechanically adjustable rather than actuated. Also, coarse and fine stroke are combined into an *XYZ*-manipulator.

Preliminary research used an experimental set-up (Figure 12) to probe a PIC (Figure 13; see also the schematic in Figure 5) with a 1x12 fiber array of pitch 250 μm. A theoretical model was also developed, incorporating the Gaussian beam approximation and fiber-array dimensions.
The results showed that the *Rx* and *Ry* can be made passive, with tolerances of *Rx* < 62 mrad and *Ry* < 9 mrad. The *Rz* (probe roll axis) tolerance is much stricter, with a requirement of < 1 mrad, which can be compensated by the wafer stage's *Rz* DoF. It should be noted that the error budget currently allocates ~1 dB to the *XYZ*-axes and 2.6 dB per rotational axis. Further research will focus on reallocating the error budget for specific use cases and development of the prototype design of this alignment concept.

Collision avoidance

A concept for collision avoidance during trench coupling utilises a periscope probe, as shown in Figure 7, with additional channels facing in other directions for multi-DoF measurements. It measures gap distances by analysing reflections from both the probe itself and the PIC.

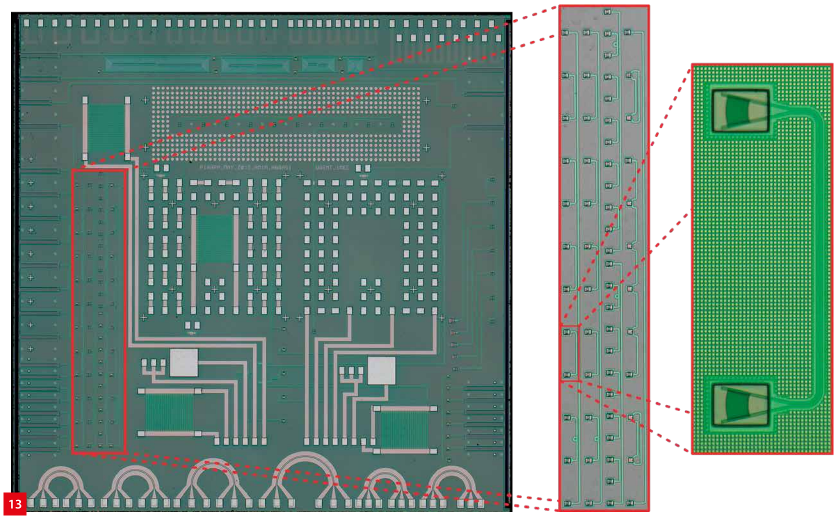

13

The reference PICs were designed and fabricated as part of the Pixapp Pilot Line, utilising the imec iSiPP50G platform to demonstrate advanced photonic packaging processes [2].

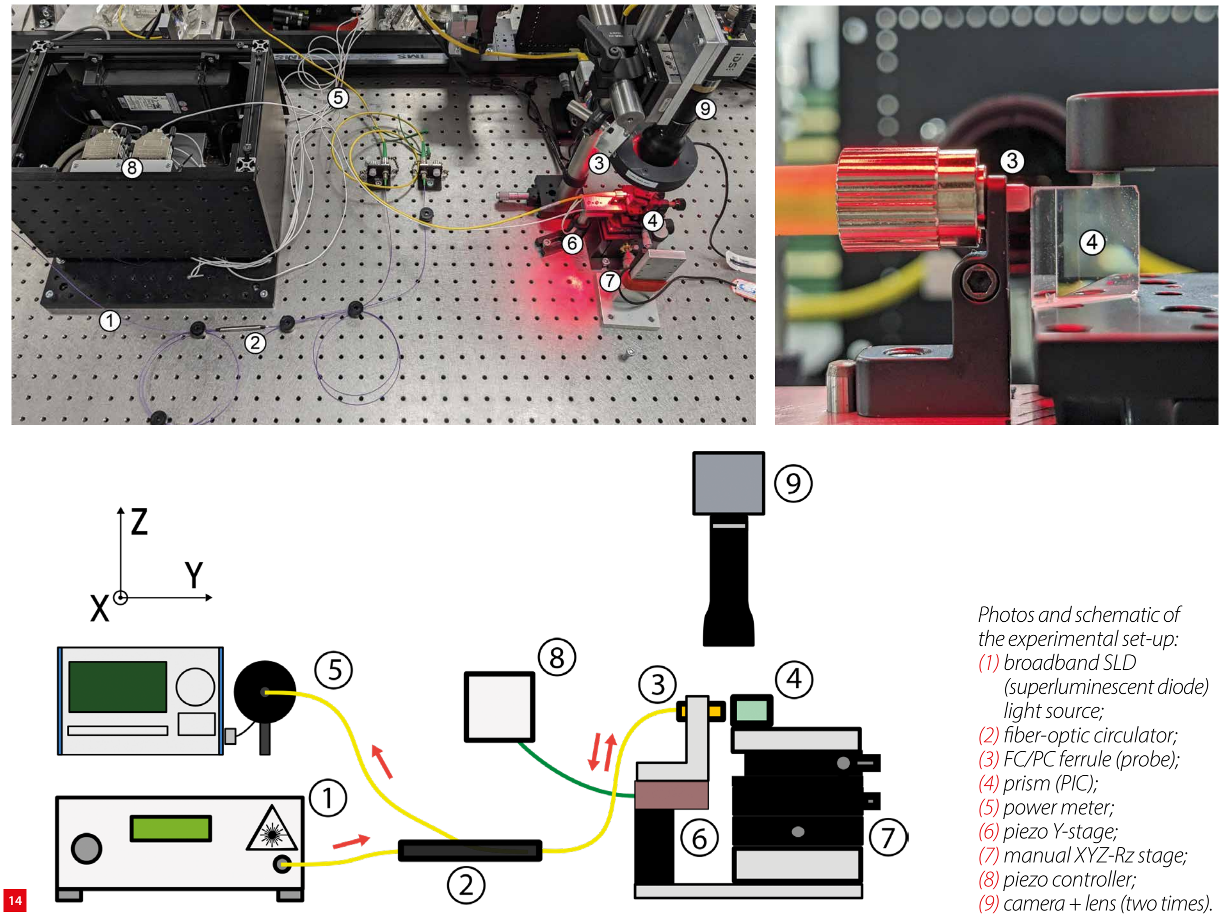

14

Photos and schematic of the experimental set-up:
(1) broadband SLD (superluminescent diode) light source;
(2) fiber-optic circulator;
(3) FC/PC ferrule (probe);
(4) prism (PIC);
(5) power meter;
(6) piezo Y-stage;
(7) manual XYZ-Rz stage;
(8) piezo controller;
(9) camera + lens (two times).

The feasibility of this concept was researched with an experimental set-up as shown in Figure 14. The probe and PIC are mimicked with a ferrule and a glass prism, respectively. Using a piezo stage, the ferrule is precisely actuated with respect to the prism in a single DoF.
A broadband light source is connected to the ferrule with in between a circulator. The reflected light is guided to another port of the circulator, which is connected to a power meter. The measured reflected light intensity is compared with the relative position of the encoder of the piezo and validated with a camera + lens system. Besides, the upper and lower envelope are determined by model-based fitting.

The fitted parameters are the transmissivity of the ferrule-air and air-glass interfaces, the Rayleigh length and the standard deviation of the power spectrum. In addition, a parameter is included to shift the fitted envelopes horizontally, to account for difficulties with determining zero-gap size.

The measured near-field reflected intensity profile and fitted envelopes are shown in Figure 15. The overall shape was as expected. The interference pattern is only visible for a gap distance smaller than 40 μm. Furthermore, the intensity goes towards a constant, non-zero value, normalised to one in the far-field region, as shown in Figure 16.

Initial results showed that the reflected light's intensity profile can be model-based fitted with an accuracy of 2-3 μm and a repeatability of 1.5 μm. The error is primarily due to non-parallel surfaces, determining the zero-gap size, as well as varying reflections and malfunctioning of the piezo-encoder combination.

Further research will focus on repeating the measurements with a more reliable piezo-encoder combination and implementing this concept with multiple DoFs into a periscope probe and coupling with a PIC.

REFERENCES

[1] D. Marcuse, "Loss analysis of single-mode fiber splices", *Bell System Technical Journal*, vol. 56 (5), 1977.
[2] Pixapp, "Standardisation", *pixapp.eu/technology/standardisation*, (accessed 1-12-2024).
[3] Physik Instrumente, "Fast, Multi-Channel Gradient Search Routines", *www.physikinstrumente.com/en/products/fast-multi-channel-photonics-alignment-systems/r-fmp-gsm-fast-multi-channel-gradient-search-routines-412418477*, (accessed 3-12-2024).
[4] R. Polster, *et al.*, "Wafer-scale high-density edge coupling for high throughput testing of sillicon photonics", *Optical Fiber Communication Conference*, San Diego, 2018.
[5] M. Trappen, *et al.*, "3D-printed optical probes for wafer-level testing of photonic integrated circuits", *Optics Express*, vol. 28 (25), 2020.
[6] S. Khan, *et al.*, "Low-loss, high-bandwidth fiber-to-chip coupling using capped adiabatic tapered fibers," *APL Photonics*, vol. 5 (5), 2020.
[7] X. Leijtens, R. Santos, and K. Williams, "High Density Multi-Channel Passively Aligned Optical Probe for Testing of Photonic Integrated Circuits", *IEEE Photonics Journal*, vol. 13 (1), pp. 1-15, 2021.

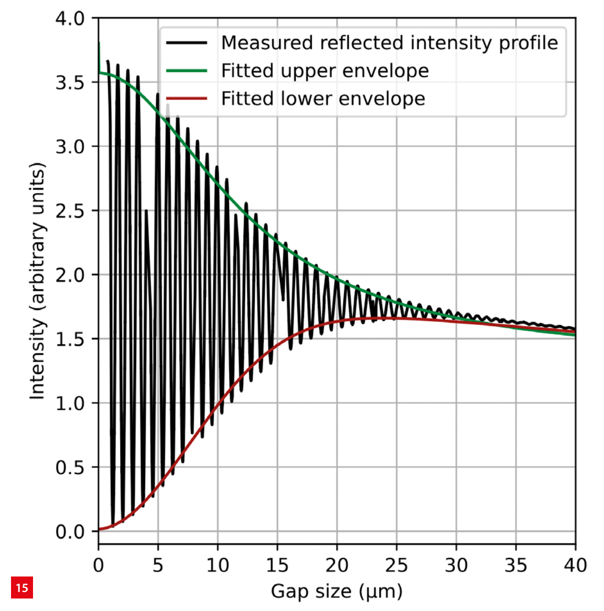

15

Measured (near-field) reflected intensity profile with model-based fitted upper and lower envelopes. The discontinuities are due to the slipping of the piezo-encoder combination.

[8] eazy works, "EZ-MES", *www.eazyworks.com* (accessed 22-1-2025).
[9] L. Mulder, "Investigating the effect of misalignment on the efficiency of fiber array to grating coupling to support the design of a sophisticated passive DOF alignment system", University of Twente, M.Sc. thesis, 2023.
[10] A. Heijink, "Collision Avoidance for Trench Coupling using Photonic Probe-Chip Reflections", University of Twente, M.Sc. thesis, 2024.

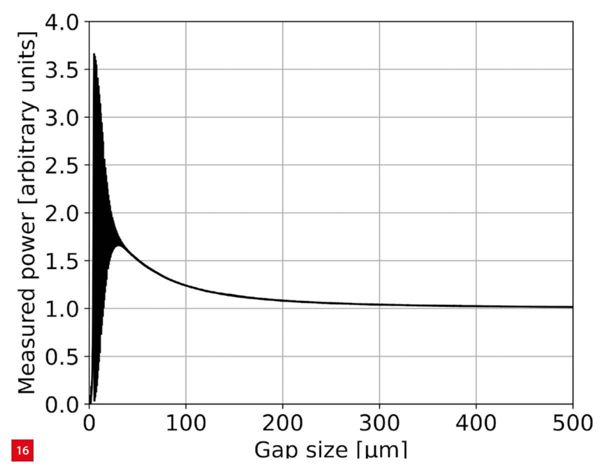

16

Measured (far-field) reflected intensity profile.

VIDEO
[V1] IMS, "360-view of Photonic Test Prober SIRIUS", *https://youtu.be/egfNyLE8is4*